



HAL
open science

Reactivity of beryllium in aqueous solution from acidic to basic pH

Céline Cannes, Pauline Bouhier, David Lambertin, Christian Grisolia, Davide Rodrigues, Sylvie Delpech

► **To cite this version:**

Céline Cannes, Pauline Bouhier, David Lambertin, Christian Grisolia, Davide Rodrigues, et al.. Reactivity of beryllium in aqueous solution from acidic to basic pH. *Journal of Electroanalytical Chemistry*, 2023, 950, pp.117879. 10.1016/j.jelechem.2023.117879 . hal-04337647

HAL Id: hal-04337647

<https://hal.science/hal-04337647v1>

Submitted on 24 Oct 2024

HAL is a multi-disciplinary open access archive for the deposit and dissemination of scientific research documents, whether they are published or not. The documents may come from teaching and research institutions in France or abroad, or from public or private research centers.

L'archive ouverte pluridisciplinaire **HAL**, est destinée au dépôt et à la diffusion de documents scientifiques de niveau recherche, publiés ou non, émanant des établissements d'enseignement et de recherche français ou étrangers, des laboratoires publics ou privés.

Reactivity of beryllium in aqueous solution from acidic to basic pH

Céline Cannes,^{1*} Pauline Bouhier,^{1,2} David Lambertin,² Christian Grisolia,³ Davide Rodrigues,¹ Sylvie Delpech¹

1 Université Paris-Saclay, CNRS/IN2P3, IJCLab, 91405 Orsay, France

2 CEA, DES, ISEC, DE2D, SEAD, Université de Montpellier, Bagnols-sur-Cèze, France

3 CEA, IRFM, Saint Paul-lez-Durance, France.

Keywords

Beryllium, reactivity, thermodynamic data, pH measurement, electrochemical impedance spectroscopy.

Abstract

Beryllium wastes produced by nuclear industry could be managed by encapsulation in cements. The main risk is the aqueous corrosion, which leads to the hydrogen production and cracks causing a loss of radioactivity confinement. However, the corrosion can be limited by the formation of the hydroxide solid phase $\text{Be}(\text{OH})_{2(s)}$. A study on the influence of the pH on the reactivity of beryllium was carried out in aqueous solution. The solubility diagram was first drawn with the recent thermodynamic data to confirm the stability domain of the different beryllium forms and to calculate their solubility depending on the pH of the solution. The results showed that the hydroxide solid phase is stable until very high basic pH of 14. The pH variation of solution at different initial pH was measured after immersion of metallic beryllium. The results are in good agreement with the calculated solubility diagram. The electrochemical impedance spectra were also recorded at a beryllium electrode from pH 2 to 15. The Nyquist and Bode diagrams were fitted by using an electric equivalent circuit. This study allowed to evaluate the Be reactivity by measuring the charge transfer resistance as a function of the pH. Again, the results confirm that the corrosion of beryllium is limited at neutral to basic pH and

this low reactivity was attributed to the formation of the hydroxide solid phase $\text{Be}(\text{OH})_2$. Moreover, the EIS study put in evidence that the corrosion of beryllium is the lowest in solutions having pH around 12. In this pH range, the Be metal would be protected against the corrosion both by the formation of the hydroxide solid $\text{Be}(\text{OH})_2$ and by the adsorption of hydroxide ions (OH^-) at the metal surface.

1. Introduction

Beryllium (Be) presents interesting properties, such as a low density, a relatively high melting point (1287 °C), a low neutron-capture cross section and a high neutron scattering cross section, a high specific heat and thermal conductivity, good mechanical properties at elevated temperatures and high oxygen gettering characteristics [1]. It is then employed in a wide range of applications and especially in nuclear industry. Be metal is currently employed in thermal reactors as a moderator, a reflector or fuel cladding [2-5]. It is also under study as interesting material for the future fusion power reactors. In the International Thermonuclear Experimental Reactor (ITER), Be constitutes the main plasma facing for the first wall of the tokamak and the neutron multiplier in the breeding blanket [6-10].

Since beryllium is used in fission and fusion reactors, low- and intermediate-level radioactive metallic Be wastes are generated. Concrete encapsulation is one strategy to manage this type of metallic wastes by isolating them from the environment [11-13]. Metallic wastes produced by nuclear activities are various and, under certain circumstances, they can react with cement phases or aqueous interstitial solution, thus reducing the quality of the conditioning material. The major risk is the oxidation of the metal by the interstitial water, resulting in the hydrogen release. This can lead to gas driven transport of radionuclides out of the waste package. The confinement is no longer ensured. Currently, research is conducting to develop alternative cementing systems for the encapsulation of problematic low and intermediate level metal radioactive waste. The pH of the pore solution strongly influences the reactivity of the metal in the matrices. Whatever the pH, in aqueous solutions, metallic wastes are generally not stable and they are oxidized by water. However, in given pH domains, the metal can be oxidized to oxide or hydroxide compound in solid state, forming a coating at the metal surface. This passivation layer protects the metal against corrosion and the hydrogen produced by water reduction is limited. The degree of protection against corrosion is function of the stability and adherence of the passivating layer. To ensure a safety storage, it is then primordial to understand the reactivity of the metallic nuclear wastes in aqueous solution as a function of the pH.

Beryllium presents a very high toxicity. Beryllium in powder form is known as carcinogen and it can cause an incurable respiratory disease, the berylliosis [14, 15]. This may explain the few works on the chemistry of this element. Some corrosion studies are nevertheless reported in the literature [16-22] which show that beryllium is highly corrosion resistant in water at low temperature. Moreover, these studies have also shown that impurities at the surface can cause local corrosion [23] and the presence of aggressive anions in solution, such as chloride ions, can generate pitting corrosion [24-27]. The metal is protected by a layer of oxide BeO or hydroxide solid phase Be(OH)₂ of 20 to 100 angstroms thickness, when exposed to air. The reactivity of beryllium is mainly related to the stability of this protective layer. In acid solutions, the dissolution of the solid oxide layer is extensively proven, leading to a continuous corrosion of the metal. By contrast, in alkaline to hyperalkaline solutions, the studies on the solubility of the beryllium oxide or hydroxide solid phase are more controversial. While oldest studies based on thermodynamic calculation predict in alkaline solution the formation of anionic species, such as Be₂O₃²⁻ [28], more recent studies show that the predominant species in alkaline to hyperalkaline (NaOH 5 mol.L⁻¹) solutions are Be(OH)₂, Be(OH)₃⁻ and Be(OH)₄²⁻ [29]. As anionic species have been formed in alkaline media, beryllium is not protected against the corrosion by a passivation layer. In such conditions, the corrosion is continuous. Although some experimental studies have shown a strong uptake of Be(II) species in low and high alkaline cementitious matrices, according to the thermodynamic data, the beryllium corrosion could lead to a continuous production of hydrogen gas, which can compromise the nuclear waste confinement [30, 31]. A previous study was realized on the evaluation of several cementitious matrices to condition Be wastes [32] and the E-pH diagram of Be was first calculated in water by considering the recent published thermodynamic data. This calculation has shown that from 5.3 to 13.5 at a concentration of 10⁻⁴ mol.L⁻¹, the predominant form of beryllium is the hydroxide solid phase Be(OH)₂. For pH more acid or more basic, ionic forms of Be(II) are stable. A qualitative electrochemical study was also carried out to follow the reactivity of beryllium in different types of cement. The results showed that beryllium nuclear waste can actually be conditioned in a Portland cement, a calcium sulfoaluminate cement (characterized by a basic pore water solution) or a magnesium phosphate cement, which has a neutral pore water solution after several days of hydration. However, in magnesium phosphate cement a corrosion is observed during the first days, while in Portland cement the beryllium is highly passivated during the entire studied time range.

As the reactivity of beryllium depends mainly on the formation and the properties of the hydroxide solid phase $\text{Be}(\text{OH})_2$, we have carried out a study on the reactivity of Be in solution from acidic to basic pH. The solubility diagram has been drawn with the recent thermodynamic data to establish the stability domain of the different beryllium forms and to calculate their solubility depending on the pH of the solution. Experimental studies have also been carried out. First, the variation of the pH of solutions containing beryllium metal has been measured as a function of time. Then, the reactivity of beryllium has been studied by electrochemical impedance spectroscopy in acidic to highly alkaline solutions by using electric equivalent circuit model. The experimental results have been compared to the ones presented in the solubility diagram.

2. Experimental section

2.1. Chemical products and solutions preparation

The solutions at pH 2, 3.2 and 4.3 were prepared by dilution of HCl solution (35 or 37% from VWR Chemicals). The solutions at pH from 5.9 to 10.7 were prepared by addition of small volume of NaOH solution to the solution at pH 4.3. The solutions at pH 12 to 14 were prepared by dilution of 10.0 mol.L^{-1} NaOH solution (Honeywell™ Fluka™ from Fisher Scientific). The basic solution called “pH 15” corresponds to the NaOH solution at 10 mol.L^{-1} . After opening the bottle of 10 mol.L^{-1} NaOH, it was stored in a desiccator maintained under argon to prevent carbonation.

2.2. pH measurements

The pH measurements were carried out with a Consort C3010 pH meter and a Mettler Toledo Inlab Expert Pt1000 pH probe. Calibration was performed with IUPAC pH standard solutions 1.68 – 4.00 – 6.86 – 10.01 and 12.45 (± 0.01).

For the NaOH solutions with a concentration higher than 1 mol.L^{-1} , the concentration of the hydroxide was determined by titration with a $10^{-2} \text{ mol.L}^{-1}$ HCl solution.

2.3. Electrochemical Impedance Spectroscopy measurements

A three-electrode cell was used for the electrochemical measurements, with a working electrode (beryllium wire), a counter electrode (platinum wire) and a quasi-reference electrode (platinum wire). The electrochemical set-up is reported Figure 1. It is under controlled atmosphere

(Synthetic air, N₂/O₂ 80/20 vol.%) to avoid pH variation by carbonation of the solutions. This set-up is also used to measure the variation of the pH of the solution with time.

The beryllium wire (1.2 mm diameter, Goodfellow, purity 99.7%) was cut and cleaned by rinsing with ethanol and was pickled with a HCl (0.5 M) solution until a light grey appearance (around 1 min). Then it was rinsed thoroughly with demineralized water and dried with a tissue paper. The surface of the beryllium working electrode in solution is 0.765 cm².

The Pt wire (diameter: 1 mm, Goodfellow, purity 99.9%) was cut and cleaned with ethanol and heated until bright-red color with a blowtorch. The surface of the Pt electrode in solution is 1.26 cm².

As beryllium powder is highly toxic, the Be wire was stored and handled under a glove box, in case of formation of powder during its handling.

Measurements were carried out using a potentiostat (AMETEK model VersaSTAT 4) piloted by the VersaStudio software. Electrochemical Impedance Spectroscopy (EIS) diagrams were recorded at the open circuit potential with 20 mV amplitude. Frequency ranged between 10⁵ and 10⁻¹ Hz, with 10 frequencies values per logarithmic decade. The electrochemical impedance spectra were fitted with the Zview software.

3. Results and discussion

3.1. Thermodynamic data calculations

Based on the thermodynamical database selected in ref [32], the solubility diagram of Be(II) in water has been calculated in water at 25°C as a function of the pH by using the expression of the acid-base equilibrium constants reported Table 1. The solid form of Be is Be(OH)₂ which can dissolve into 6 different forms depending on pH (Fig.2).

This figure shows that the best pH domain for stabilizing the solid layer corresponds to the lower solubility of Be(OH)₂, that is a pH ranging between 8.2 and 10.5. However, the passivating properties of a solid layer depends both on the nature of the layer and on its adherence and homogeneity. Only experimental measurements make it possible to conclude that a passivating layer has formed and to evaluate its degree of protection against corrosion.

3.2. Experimental pH measurements

The thermodynamic data are really helpful to define the possible reactions, including acid-base reactions and redox reactions, and consequently the different stable chemical forms depending

on the conditions (pH, potential, total concentration of the species). However, to confirm the reactivity of a metallic species, experimental studies are primordial.

In this context, we have carried out a study on the pH variation of a solution containing metallic beryllium. As it was shown in the thermodynamic calculations, no domain of immunity of Be(0) is observed in aqueous solution and the reaction of dissolution of Be metal in aqueous solution depends on the pH range.

The several dissolution reactions expected are:

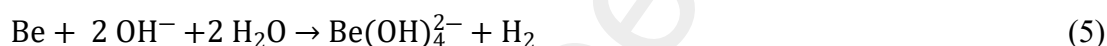
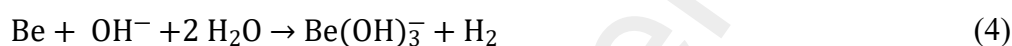
For $\text{pH} < 8$:



For $8 < \text{pH} < 10.5$:



For $\text{pH} > 10.5$:



The formation of Be^{2+} and BeOH^+ leads to an increase of pH due to the consumption of H^+ and the formation of $\text{Be}(\text{OH})_3^-$ and $\text{Be}(\text{OH})_4^{2-}$ to a decrease of pH due to the consumption of OH^- .

The domain of formation of $\text{Be}(\text{OH})_2$ (for pH ranging between 8 and 10.5) is the only one for which no modification of pH occurs during the dissolution reaction. It does not mean that the dissolution is stopped but means that the solubility of Be(II) is reached. In these conditions, Be is oxidized to Be(II) which precipitates at the surface under $\text{Be}(\text{OH})_2$ solid. This precipitate can be protective or not against corrosion, but in the two cases, the pH remains constant with time. The set-up presented Figure 1 has been used to measure the pH evolution of a solution containing beryllium metal. This cell is maintained under controlled gaseous phase (synthetic air, N_2/O_2 80/20 mol%) to avoid the carbonation of the solutions (and consequently the pH variation of them by this reaction). For an initial pH of 3, Figure 3 shows an increase of the pH of the solution with time until a plateau value around 5.9. This evolution is consistent with the reactions (1) and (2) corresponding to the formation of Be^{2+} or $\text{Be}(\text{OH})^+$. According to the reactions (1) and (2), the concentration of beryllium in solution can be calculated, since in the first case, the formation of one mole of Be(II) involves the consumption of two moles of protons (reaction (1)) or one mole of protons (reaction (2)). As it is mentioned previously, the pH becomes constant when the solubility of Be(II) is reached. If we consider the formation of the

Be²⁺ cation, the final concentration of Be(II) is $5.31 \cdot 10^{-4} \text{ mol.L}^{-1}$, while if we consider the formation of Be(OH)⁺ cation, the final concentration of Be(II) is $5.33 \cdot 10^{-4} \text{ mol.L}^{-1}$. These values are quite similar. According to the diagram presented Figure 2, a solubility of $5.3 \cdot 10^{-4} \text{ mol.L}^{-1}$ corresponds to pH 5.1. The thermodynamic data presented in this work (pH 5.1) and the experimental values (pH 5.9) are then in good agreement. The difference between the thermodynamic and the experimental values can be attributed to an overestimation of the total Be(II) concentration, since the amount of Be(OH)₂ formed has been neglected.

For an initial value of 12.9, the pH of a solution containing beryllium metal does not vary significantly with time (Fig. 3). Therefore, the reactions (4) and (5) do not take place. At this pH value, the predominant form of Be(II) is neither Be(OH)₃⁻ nor Be(OH)₄²⁻ but rather Be(OH)₂. This experimental result is in good agreement with the recent thermodynamic calculations.

The pH of a solution containing Be and having an initial pH of 14 has been also measured with a pH paper because the pH cannot be determined with the pH-meter for values higher than 13.5. During 1 day, we have not observed any significant gas evolution at the Be metal surface and any pH variation (Fig. 3). However, a loss mass of Be was measured and reported in Table 2. According to the thermodynamic data presented above, to observe a significant corrosion of beryllium, the pH of the solution has to be greater than 14.5, the lower limit of the stability domain of the anionic species Be(OH)₄²⁻. Study of the reactivity of Be in high basic solutions was realized by immersion of beryllium metal in a solution of NaOH 10 mol.L^{-1} . For hydroxide concentrations greater than 1 mol.L^{-1} , the pH of the solution has been determined considering the expression (6).

$$\text{pH} = 14 + \log [\text{OH}^-] \quad (6)$$

And the hydroxide concentration has been titrated with a $10^{-2} \text{ mol.L}^{-1}$ HCl solution by using the pH-meter. After immersion of Be, significant gas evolution has been observed at the Be metal surface during more than 3 days. This observation confirms the thermodynamic data: at pH 15, beryllium metal is highly corroded to an anionic species. The aqueous dissolution is continuous, the metal cannot be protected by the hydroxide solid phase Be(OH)₂, which is not stable at this pH. As soon as there is no longer any gas formed, the concentration of hydroxide ions was titrated and the mass of the beryllium wire measured. The pH of the solution has decreased from pH 15 to 14.95 and the corresponding mass loss of beryllium was 0.109 g.

For each experiment, the values of the final pH and the corresponding mass loss of beryllium have been reported Table 2. The mass loss corresponds to the total amount of oxidized beryllium. The total concentration of Be(II) could then be calculated. We have added the

different values (pH_f , $\log [\text{Be(II)}]$) of the Table 2 on the speciation diagram (Fig. 2). At basic pH, these values are in good agreement with the recent thermodynamic data. The points are in agreement with the solubility of Be(OH)_2 as a function of pH.

The pH evolution in acidic solution is characteristic of the dissolution of beryllium metal. The plateau reached corresponds to the precipitation of Be(OH)_2 . The protective character of Be(OH)_2 cannot be deduced from this experiment because the constant value of pH can be due (i) to the stop of the dissolution by precipitation of Be(OH)_2 at the Be metal surface and protection of the metal hydroxide and (ii) to a continuous dissolution of Be to Be(OH)_2 (which can precipitate in the solution bulk), this reaction involving no pH variation.

The passivating/protective character of Be(OH)_2 has been examined by electrochemical measurements.

3.3. Electrochemical Impedance Spectroscopy measurements

Electrochemical Impedance Spectroscopy is an interesting technique for understanding the reactivity of redox compounds and for accessing to data on the electrolyte/metal interface. The formation of a passive layer can be observed and the degree of passivity against the metal corrosion can be evaluated by this technique. Moreover, if the EIS is recorded at the OCP, this technique presents the advantage not to alter the medium/metal interface. The electrochemical impedance spectra, in Nyquist and Bode representations, have been recorded on a beryllium electrode in aqueous solution from pH 2 to 15.

The corrosion of a metal can be limited by the formation of a passivation layer. The degree of protection against the corrosion depends on the characterization of this solid phase: adherence, solubility, thickness, compacity, porosity in the studied media. All of these parameters are function of the chemical composition of the media, the pH value but also the presence of some chemical compounds. Since our goal is to study specifically the effect of pH on the reactivity of beryllium and because chemical compounds mainly used as pH buffers can affect the reactivity of the metal, the solutions at different pH values have been prepared by using only HCl and NaOH solutions (see experimental section). Pitting corrosion of beryllium in aqueous solutions in presence of chloride ions has been reported in the literature. However, this phenomenon occurs at high chloride concentration and it is favored by impurities at the metal surface and the crystallographic orientation of the metal [19, 20, 23, 27]. For that reasons, the concentration of chloride ions have been limited to $10^{-2} \text{ mol.L}^{-1}$ and a high purity of the metal (99.7%) has been selected for this work.

The Nyquist and Bode diagrams recorded on Be electrode in aqueous solutions are presented Figure 4 (the points represent experimental measurements and the lines correspond to the simulation of the diagrams). At pH 2, a significant gas evolution is observed near the electrode which confirms the thermodynamic data and the previous studies in acidic solutions. The impedance diagrams put in evidence an inductive effect for frequencies lower than 10^3 Hz. This can be attributed to the cathodic production of hydrogen gas by aqueous corrosion of beryllium. A mechanism of this reaction was first proposed by Volmer-Heyrovsky [37]. It includes two successive mono-electronic transfers with an intermediate adsorbed species.

In solutions from pH 3.2 to 5.9, a capacitive loop attributed to the charge transfer is observed at high frequencies. At intermediate and low frequencies, a straight line with a phase angle of 45° characteristic of diffusion impedance is observed. The charge transfer characterizes the corrosion reaction (oxidation of Be and reduction of H_2O). For this pH range, Be is corroded and the reaction is limited by the diffusion of the oxidizing agent. No passivation process, related with the formation of a solid layer at the surface of Be is observed.

In solutions from pH 6.2 to 12, the impedance increases and tends to very high values in the solutions at pH close to 12. This can be explained by the passivation of the beryllium metal with formation of a solid layer at its surface, the degree of protection against the corrosion being the highest at pH 12.

From pH 13 to “pH 15”, corresponding to the 10 mol.L^{-1} NaOH solution, the Nyquist diagram is characterized by a single capacitive loop with a resistance decreasing when the pH increases. This behavior is the same as the one observed in solution at pH 2, corresponding to a continuous corrosion with production of hydrogen. No diffusion process and no inductive effect are evidenced, the inductive effect being related to the adsorption of protons which are not involved in the reaction at high pH values.

To determine the reactivity of Be in solution as a function of the pH, the electrochemical impedance spectra have been simulated by using an electric equivalent circuit (Figure 5). Pure capacitances are replaced in this circuit by Constant Phase Element (CPE) as it was suggested by MacDonald [38] and Brug et al. [39] to consider the heterogeneity of the electrolyte/metal interface. The impedance of CPE is given by:

$$Z_{CPE} = \frac{1}{K(j\omega)^\alpha} \quad (7)$$

in which K ($F.s^{\alpha-1}$) is a constant, j the complex number ($j^2 = -1$), ω the pulsation and α a coefficient generally ranging between 0.8 and 1 (1 corresponding to a pure capacitance).

The resistance R_e (Ω) represents the resistance of electrolyte. The electrical circuit $CPE_L//R_L$ is the circuit used to model the passivating layer. CPE_{dl} models the double layer capacitance and R_{ct} the charge transfer resistance. Z_W is the Warburg impedance characteristic of the diffusion process [40] and its expression is given by:

$$Z_W = \frac{R \times \tanh(j\omega T)^p}{(j\omega T)^p} \quad (8)$$

in which, R is a constant expressed in Ω , T is a term which depends on diffusion parameters such as D and δ being respectively the diffusion coefficient (cm^2/s) and the diffusion layer thickness (cm) and p is a coefficient close to 0.5 [41].

The circuit R_{ads}/L_{ads} represents the inductive effect related to the proton adsorption observed at pH 2. All the diagrams have been fitted using the same electrical circuit but depending on the pH domain, some electrical parameters were voluntarily not considered by fixing their impedance to 0.

The electrochemical impedance spectra have been fitted with the Zview software. Figure 4 presents the fit for each pH (black lines) and the values of the different electrical parameters are reported Table 3.

The electrical circuit chosen leads to fit correctly the impedance diagrams. Even if it is simplified (it does not consider the two charge transfer resistances obviously involved in the mechanism and related to the oxidation of Be and to the reduction of H_2O), the charge transfer resistance is inversely proportional to the corrosion current. The variation of R_{ct} with pH is presented Figure 6. This resistance has the lowest values for pH below 6 and greater than 14. That means that for this pH ranges, $\text{pH} < 6$ and $\text{pH} > 14$, beryllium metal is highly corroded. That is in agreement with the thermodynamic data, Be being oxidized into cationic species, Be^{2+} and $\text{Be}_3(\text{OH})_3^{3+}$, in acid solutions and into anionic species, $\text{Be}(\text{OH})_4^{2-}$, in highly basic solutions. For pH comprised between 6 and 14, the values of R_{ct} are large. The corrosion of beryllium metal is limited by the formation of the hydroxide solid phase $\text{Be}(\text{OH})_2$, which is thermodynamically stable in this pH range. Close to pH 12, a strong increase of R_{ct} is observed, characteristic of a very high passivation of the electrode. Neither the thermodynamic calculations nor the study of the pH variation have made it possible to anticipate this phenomenon. It is unlikely due to the formation of another solid compound, since the literature does not mention any other solid phase than $\text{Be}(\text{OH})_2$. However, one can suggest an increased passivation due to an adsorption of hydroxides on the surface of the passivation layer and which would provide an additional resistance. At higher pH, the stability of the $\text{Be}(\text{OH})_2$ layer decreases to form soluble hydroxides, Be metal is no longer protected by the hydroxide solid

phase against the corrosion. The role of hydroxides on the passivation of oxide layers was already shown in the case of uranium behavior as a function of pH [42].

Conclusion

Due to its specific properties, beryllium is a metal compound used in the nuclear industry. The management of Be nuclear waste has to be considered. One way to manage this type of waste is the encapsulation in a cement. The pH of the pore water solution of the conditioning matrices strongly influences the reactivity of the metal waste. To select the best matrices to manage Be waste, it is then primordial to understand the reactivity of this metal depending on the pH of the medium.

In this context, the reactivity of beryllium in water has first been studied by a thermodynamic approach. The solubility diagram of Be was calculated as a function of the pH. This diagram shows a large stability domain of the hydroxide solid phase, which spreads until very high basic values. According to this thermodynamic study, Be metal can be protected against the corrosion by the formation of $\text{Be}(\text{OH})_2$, its solubility being very low, close to 10^{-6} M between pH 6 and 12.

Experimental studies have also been carried out. The pH of solutions containing beryllium metal have been measured. The results confirm that in acid solutions, Be is oxidized into Be^{2+} . Then, in this pH range, the corrosion reaction involves the consumption of protons. The pH increases until reaching the pH of $\text{Be}(\text{OH})_2$ precipitation, around pH 6. By contrast, if Be metal is immersed in a solution of pH 13 and 14, the pH remains constant on a period of several days. That means that Be is oxidized to $\text{Be}(\text{OH})_2$ (no pH evolution) which passivates the electrode surface in alkaline solution. To observe a pH variation and gas evolution on the Be surface in the alkaline domain, the initial pH of the solution has to be “15” (corresponding to 10 mol.L^{-1} NaOH solution). The pH of this solution decreases until pH 14.95, corresponding to the pH of $\text{Be}(\text{OH})_2$ precipitation.

The reactivity of Be in aqueous solutions has also been studied by electrochemical impedance spectroscopy to evaluate the degree of protection of the hydroxide solid phase against the corrosion as a function of the pH. The Nyquist and Bode diagrams have been fitted by using an electric equivalent circuit. The EIS simulations made it possible to evaluate the reactivity of Be as a function of the pH of the solution by determining a charge transfer resistance inversely proportional to the corrosion current. The results confirm both the thermodynamic calculation and the study of pH evolution by immersion of Be metal: Be is oxidized in acid solutions until

pH 6 and in very alkaline solution. This study has also put in evidence a passivation zone from pH 6 to 14, the passivation being the most efficient for pH close to 12. This phenomenon has been explained by a higher protection of the metal surface by hydroxide adsorption instead of a different chemical composition of the passive layer.

In the context of metallic waste management, these results are very important since the mainly used conditioning matrices present basic pore water solution.

Author information

Corresponding author: celine.cannes@ijclab.in2p3.fr / 33 1 69 15 71 52

IJCLab, Université Paris-Saclay, CNRS/IN2P3, 15 rue Georges Clémenceau, 91405 Orsay cedex, France

References

- [1] K. A. Walsh, Beryllium chemistry and processing, 2009, ASM International.
- [2] H. Pih, A survey of beryllium technology and nuclear applications, ORNL-4421 report 1969.
- [3] J.M. Beeston, Nucl. Eng. Des. 14 (1970) 445-474.
- [4] L.L. Snead, S.J. Zinkle, AIP Conference Proceeding 746 (2005) 768.
- [5] D. Chandler, G.I. Maldonado, L.D. Proctor, R.T. Primm, Nucl. Tech. 177 (2012) 395-412.
- [6] J.S. Park, X. Bonnin, R. Pitts, Nucl. Fusion 61 (2021) 016021-01636.
- [7] J.H. Kim, S. Nakano, M. Nakamichi, J. Nucl. Mater. 542 (2020) 152522-152529.
- [8] D.L. Smith, W. Daenner, G. Kalinin and H. Yoshida, J. Nucl. Mater. 179-181 (1991) 1185-1188.
- [9] J.H. Kim, M. Nakamichi, J. Nucl. Mater. 453 (2014) 22-26.
- [10] E. Pajuste, G. Kizane, I. Igaune, L. Avotina, Jet Contributors, Nucl. Mater. and Energy 19 (2019) 131-136.
- [11] J. Li, J. Wang, J. Hazard. Mat. B 135 (2006) 443-448.
- [12] F. Glasser, Application of inorganic cement to the conditioning and immobilisation of radioactive wastes, in Handbook of advanced radioactive wastes conditioning technologies, 2011 p. 67-135.
- [13] N.B. Milestone, Adv. Appl. Ceram. 105 (2006) 13-20.
- [14] A. Seidler, U. Euler, J. Muller-Quernheim, K.I. Gaede, U. Latza, D. Groneberg, S. Letzel, Occup. Med. C 62 (2012) 506-513.
- [15] S.D. Dai, G.A. Murphy, F. Crawford, D.G. Marck, M.T. Falta, P. Marrack, J.W. Kappler, A.P. Fontenot, Proc. Natl. Acad. Sci. 107 (2010) 7425-7430.
- [16] V.D. Scott, G.V.T. Ranzetta, J. Nucl. Mater 9 (1963) 277-289.
- [17] E.T. Shapovalov, V.V. Gerasimov, Soviet Atomic Energy 26 (1969) 498-502.
- [18] E. Gulbrandsen, A.M.J. Johansen, Corr. Sci. 36 (1994) 1523-1536.
- [19] M.A. Hill, D.P. Butt, R.S. Lillard, J. Electrochem. Soc. 145 (1998) 2799-2806.
- [20] A. Venugopal, D.D. Macdonald, R. Varma, J. Electrochem. Soc. 147 (2000) 3673-3679.
- [21] F. Druyts, Fusion Eng. Des. 75-79 (2005) 1261-1264.
- [22] S. He, H. Ye, Y. Ma, L. Guo, Y. Gou, P. Zhang, Corr. Sci. 107 (2016) 21-30.
- [23] J.S. Punni, M.J. Cox, Corr. Sci. 52 (2010) 2535-2546.
- [24] M.E. Straumanis, D.L. Mathis, J. Electrochem. Soc. 109 (1962) 434-436.
- [25] K.G. Sheth, J.W. Johnson, W.J. James, Corr. Sci. 9 (1969) 135-144.

- [26] R.U. Vaidya, M.A. Hill, M. Hawley, D.P. Butt, *Metall. Mater. Trans A* 29A (1998) 2753-2760.
- [27] R.S. Lillard, *J. Electrochem. Soc.* 148 (2001) B1-B11.
- [28] M. Pourbaix, *Atlas d'équilibres électrochimiques*, Gauthier-Villars & Cie, Paris, 1963.
- [29] N. Çevirim-Papaioannou, X. Gaona, M. Böttle, E.Y. Bethune, D. Schild, C. Adam, T. Sittel, M. Altmaier, *Appl. Geochem.* 117 (2020) 104601-104612.
- [30] B. Grambow, M. Lopez-Garcia, J. Olmeda, M. Grivé, N. C.M. Marty, S. Grangeon, F. Claret, S. Lange, G. Deissmann, M. Klinkenberg, D. Bosbach, G. Bucur, I. Florea, R. Dobrin, M. Isaacs, D. Read, J. Kittnerova, B. Drtinova, D. Vopalka, N. Cevirim-Papaioannou, N. Ait-Mouheb, X. Gaona, M. Altmaier, L. Nedyalkova, B. Lothenbach, J. Tits, C. Landesman, S. Rasamimanana, S. Ribet, *Appl. Geochem.* 112 (2020) 104480-104493.
- [31] N. Cevirim-Papaioannou, I. Androniuk, S. Han, N. Ait Mouheb, S. Gaboreau, W. Um, X. Gaona, M. Altmaier, *Chemosphere* 282 (2021) 131094-131105.
- [32] P. Bouhier, C. Cannes, D. Lambertin, C. Grisolia, D. Rodrigues, S. Delpéché, *J. Nucl. Mat.* 559 (2022) 153464-153477.
- [33] P. L. Brown and C. Ekberg, Eds., *Hydrolysis of Metal Ions*. Weinheim, Germany: Wiley-VCH Verlag GmbH & Co. KGaA, 2016.
- [34] *Thermodynamic Data for Fifty reference Elements*, NASA-TP-3287, N93-19977, 1993.
- [35] E. Shock, D.C. Sassani, M. Willis, D.A. Sverjensky, *Geochim. Cosmochim. Acta* 61 (1997) 907-951.
- [36] D.N. Novak, R.V. Tilak and B.E. Conway (Eds.), *Modern Aspect of Electrochemistry*, Vol. 14, Plenum Press, New York, 1982, p. 195.
- [37] J.-P. Diard, P. Landaud, B. Le Gorrec, and C. Montella, *J. Electroanal. Chem. Interfacial Electrochem.* 255 (1988) 1-20.
- [38] J. R. MacDonald, *Solid State Ionics*, 13 (1984) 147-149.
- [39] G.J. Brug, A.L.G. Van Den Eeden, M. Sluyters-rehbach, J.H. Sluyters, *J. Electroanal. Chem.*, 176 (1984) 275-295.
- [40] A. J. Bard and L. R. Faulkner, *Electrochemical Methods: Fundamentals and Applications*, 2nd ed. John Wiley & Sons, 2000.
- [41] S. Delpéché, C. Cannes, N. Barré, Q. T. Tran, C. Sanchez, H. Lahalle, D. Lambertin, S. Gauffinet, C. Cau Dit Coumes, Kinetic model of aluminum behavior in cement matrices analyzed by impedance spectroscopy, *J. Electrochem. Soc.*, 164 (13) (2017) C717.
- [42] D. Rodrigues, C. Cannes, N. Barré, D. Lambertin, and S. Delpéché, *Electrochim. Acta* 266 (2018) 384–394.

Preprint not peer reviewed

Table 1: Expression of the acid-base equilibrium constants of the Be(II) species to calculate the solubility diagram.

Reaction	Expression of log K	Expression of log K as a function of C and pH
$\text{Be}^{2+} + \text{H}_2\text{O} \rightleftharpoons \text{BeOH}^+ + \text{H}^+$	$\log K_1 = \log \left(\frac{[\text{BeOH}^+] \times [\text{H}^+]}{[\text{Be}^{2+}] \times [\text{H}_2\text{O}]} \right)$	$\log K_1 = -\text{pH}$
$3\text{Be}^{2+} + 3\text{H}_2\text{O} \rightleftharpoons \text{Be}_3(\text{OH})_3^{3+} + 3\text{H}^+$	$\log K_2 = \log \left(\frac{[\text{Be}_3(\text{OH})_3^{3+}] \times [\text{H}^+]^3}{[\text{Be}^{2+}]^3 \times [\text{H}_2\text{O}]^3} \right)$	$\log K_2 = -2 \log C - 3 \text{pH}$
$\text{Be}^{2+} + 2\text{H}_2\text{O} \rightleftharpoons \text{Be}(\text{OH})_{2(\alpha)} + 2\text{H}^+$	$\log K_3 = \log \left(\frac{[\text{Be}(\text{OH})_{2(\alpha)}] \times [\text{H}^+]^2}{[\text{Be}^{2+}] \times [\text{H}_2\text{O}]^2} \right)$	$\log K_3 = -\log C - 2 \text{pH}$
$\text{Be}^{2+} + 2\text{H}_2\text{O} \rightleftharpoons \text{Be}(\text{OH})_{2(\text{aq})} + 2\text{H}^+$	$\log K'_3 = \log \left(\frac{[\text{Be}(\text{OH})_{2(\text{aq})}] \times [\text{H}^+]^2}{[\text{Be}^{2+}] \times [\text{H}_2\text{O}]^2} \right)$	$\log K'_3 = -2 \text{pH}$
$\text{Be}^{2+} + 3\text{H}_2\text{O} \rightleftharpoons \text{Be}(\text{OH})_3^- + 3\text{H}^+$	$\log K_4 = \log \left(\frac{[\text{Be}(\text{OH})_3^-] \times [\text{H}^+]^3}{[\text{Be}^{2+}] \times [\text{H}_2\text{O}]^3} \right)$	$\log K_4 = -3 \text{pH}$
$\text{Be}^{2+} + 4\text{H}_2\text{O} \rightleftharpoons \text{Be}(\text{OH})_4^{2-} + 4\text{H}^+$	$\log K_5 = \log \left(\frac{[\text{Be}(\text{OH})_4^{2-}] \times [\text{H}^+]^4}{[\text{Be}^{2+}] \times [\text{H}_2\text{O}]^4} \right)$	$\log K_5 = -4 \text{pH}$
$\text{Be}(\text{OH})^+ + \text{H}_2\text{O} \rightleftharpoons \text{Be}(\text{OH})_{2(\alpha)} + \text{H}^+$	$\log K_{13} = \log K_3 - \log K_1$	$\log K_{13} = -\log C - \text{pH}$
$\text{Be}(\text{OH})^+ + \text{H}_2\text{O} \rightleftharpoons \text{Be}(\text{OH})_{2(\text{aq})} + \text{H}^+$	$\log K'_{13} = \log K'_3 - \log K_1$	$\log K'_{13} = -\text{pH}$
$\text{Be}(\text{OH})^+ + 2\text{H}_2\text{O} \rightleftharpoons \text{Be}(\text{OH})_3^- + 2\text{H}^+$	$\log K_{14} = \log K_4 - \log K_1$	$\log K_{14} = -2 \text{pH}$
$\text{Be}(\text{OH})^+ + 3\text{H}_2\text{O} \rightleftharpoons \text{Be}(\text{OH})_4^{2-} + 3\text{H}^+$	$\log K_{15} = \log K_5 - \log K_1$	$\log K_{15} = -3 \text{pH}$
$\text{Be}_3(\text{OH})_3^{3+} + 3\text{H}_2\text{O} \rightleftharpoons 3\text{Be}(\text{OH})_{2(\alpha)} + 3\text{H}^+$	$\log K_{23} = 3 \log K_3 - \log K_2$	$\log K_{23} = -\log C - 3 \text{pH}$
$\text{Be}_3(\text{OH})_3^{3+} + 3\text{H}_2\text{O} \rightleftharpoons 3\text{Be}(\text{OH})_{2(\text{aq})} + 3\text{H}^+$	$\log K'_{23} = 3 \log K'_3 - \log K_2$	$\log K'_{23} = 2 \log C - 3 \text{pH}$
$\text{Be}_3(\text{OH})_3^{3+} + 6\text{H}_2\text{O} \rightleftharpoons 3\text{Be}(\text{OH})_3^- + 6\text{H}^+$	$\log K_{24} = 3 \log K_4 - \log K_2$	$\log K_{24} = 2 \log C - 6 \text{pH}$
$\text{Be}_3(\text{OH})_3^{3+} + 9\text{H}_2\text{O} \rightleftharpoons 3\text{Be}(\text{OH})_4^{2-} + 9\text{H}^+$	$\log K_{25} = 3 \log K_5 - \log K_2$	$\log K_{25} = 2 \log C - 9 \text{pH}$
$\text{Be}(\text{OH})_{2(\alpha)} + \text{H}_2\text{O} \rightleftharpoons \text{Be}(\text{OH})_3^- + \text{H}^+$	$\log K_{34} = \log K_4 - \log K_3$	$\log K_{34} = \log C - \text{pH}$
$\text{Be}(\text{OH})_{2(\alpha)} + 2\text{H}_2\text{O} \rightleftharpoons \text{Be}(\text{OH})_4^{2-} + 2\text{H}^+$	$\log K_{35} = \log K_5 - \log K_3$	$\log K_{35} = \log C - 2 \text{pH}$
$\text{Be}(\text{OH})_{2(\text{aq})} + \text{H}_2\text{O} \rightleftharpoons \text{Be}(\text{OH})_3^- + \text{H}^+$	$\log K'_{34} = \log K_4 - \log K'_3$	$\log K'_{34} = -\text{pH}$
$\text{Be}(\text{OH})_{2(\text{aq})} + 2\text{H}_2\text{O} \rightleftharpoons \text{Be}(\text{OH})_4^{2-} + 2\text{H}^+$	$\log K'_{35} = \log K_5 - \log K'_3$	$\log K'_{35} = -2 \text{pH}$
$\text{Be}(\text{OH})_3^- + \text{H}_2\text{O} \rightleftharpoons \text{Be}(\text{OH})_4^{2-} + \text{H}^+$	$\log K_{45} = \log K_5 - \log K_4$	$\log K_{45} = -\text{pH}$

Table 2: Stabilization pH, corresponding mass loss to attend this plateau value and calculation of the oxidized beryllium by considering the mass loss.

pH _f	Δm (Be) (g)	V (mL)	Log([Be(II)])
5.9	0.003	30	-1.95
6	0.001	30	-2.43
14	0.001	30	-2.43
14	0.002	30	-2.13
14.95	0.109	50	-0.61

Table 3: Set of parameters used to fit the electrochemical impedance spectra recorded on a beryllium electrode in aqueous solution at different pH. The experimental and calculated Nyquist and Bode diagrams are reported Figure 4.

pH	R_e (Ω)	CPE_L		R_L (Ω)	CPE_{dl}		R_{ct} (Ω)	Z_W			R_{ads} (Ω)	L_{ads} (Henry)
		K_L ($F.s^{-\alpha}$)	α_L		K_{dl} ($F.s^{-\alpha}$)	α_{dl}		R (Ω)	T (s)	p		
2	90	0	1	0	$3e^{-7}$	1	1	$2.05e^3$	0.011	0.52	$1.8.10^3$	10^3
3.2	$1e^3$	0	1	0	$2.5e^{-7}$	0.95	$6e^2$	$1.28e^4$	0.05	0.5	0	0
4.3	$2.1e^3$	0	1	0	$1e^{-6}$	0.95	$1.1e^3$	$6.3e^3$	0.15	0.5	0	0
5.9	$2.7e^3$	0	1	0	$1.8e^{-6}$	0.95	$1.2e^3$	$1.15e^4$	0.3	0.5	0	0
6.2	$1.98e^3$	$3.5e^{-6}$	0.93	$1.2e^3$	$1.05e^{-5}$	0.92	$1.35e^4$	$8e^3$	0.85	0.5	0	0
7.7	$1.5e^3$	$3.5e^{-6}$	0.93	$1e^3$	$1.05e^{-5}$	0.9	$1.6e^4$	$1.05e^4$	0.7	0.5	0	0
8.7	$1.5e^3$	$3.5e^{-6}$	0.93	$1e^3$	$1.05e^{-5}$	0.92	$1.3e^4$	$1.1e^4$	1	0.5	0	0
9.7	$1.3e^3$	$4.5e^{-6}$	0.93	$8e^2$	$1e^{-5}$	0.92	$1.1e^4$	$1.2e^4$	0.8	0.5	0	0
10.7	$8.5e^2$	$4e^{-6}$	0.93	$7e^2$	$1.2e^{-5}$	0.92	$9.6e^3$	$2e^4$	2.8	0.5	0	0
11.8	$1.65e^2$	$3.5e^{-5}$	0.82	$1.4e^3$	$4.35e^{-5}$	0.86	$1e^5$	0	0	0.5	0	0
12	$1.35e^2$	$1.3e^{-5}$	0.9	80	$4.1e^{-5}$	0.91	$9.8e^4$	0	0	0.5	0	0
13	14	$6e^{-5}$	0.85	$1.1e^2$	$5.75e^{-5}$	0.89	$3.5e^4$	0	0	0.5	0	0
14	1.8	$3e^{-5}$	0.9	5.5	$4.8e^{-5}$	0.95	$9e^3$	0	0	0.5	0	0
15	1.1	$2.2e^{-5}$	1	2.5	$5.5e^{-5}$	0.95	60	0	0	0.5	0	0

Figure 1: Set-up for pH measurements in solution containing beryllium and for electrochemical impedance spectroscopic measurements on beryllium working electrode, under a controlled atmosphere (N_2/O_2 , 80/20 vol%)

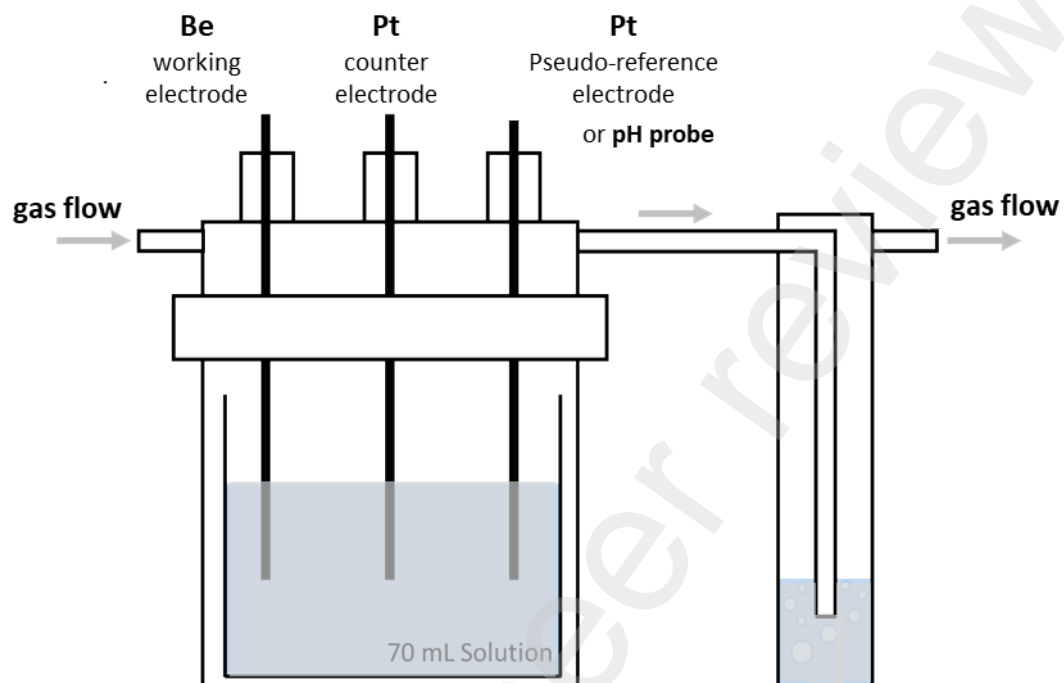


Figure 2: Solubility diagram of Be(II) species calculated in water at 25°C as a function of the pH.

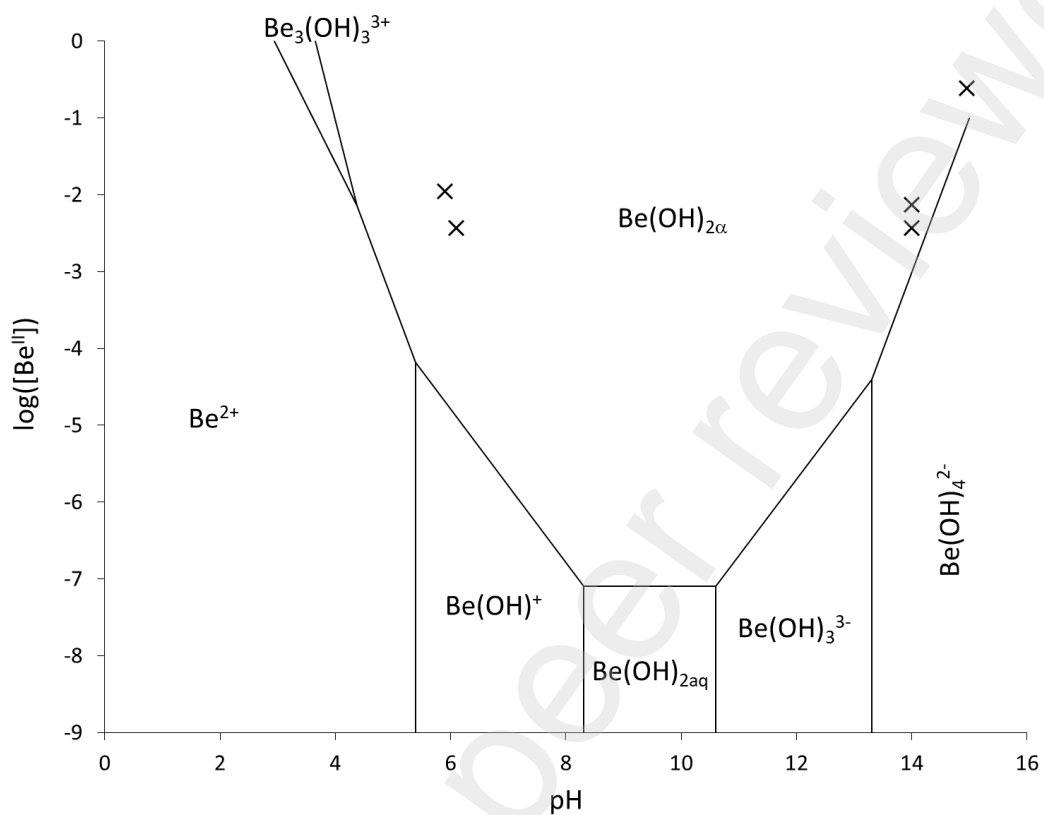


Figure 3: Variation as a function of time of the pH of solutions containing beryllium metal.

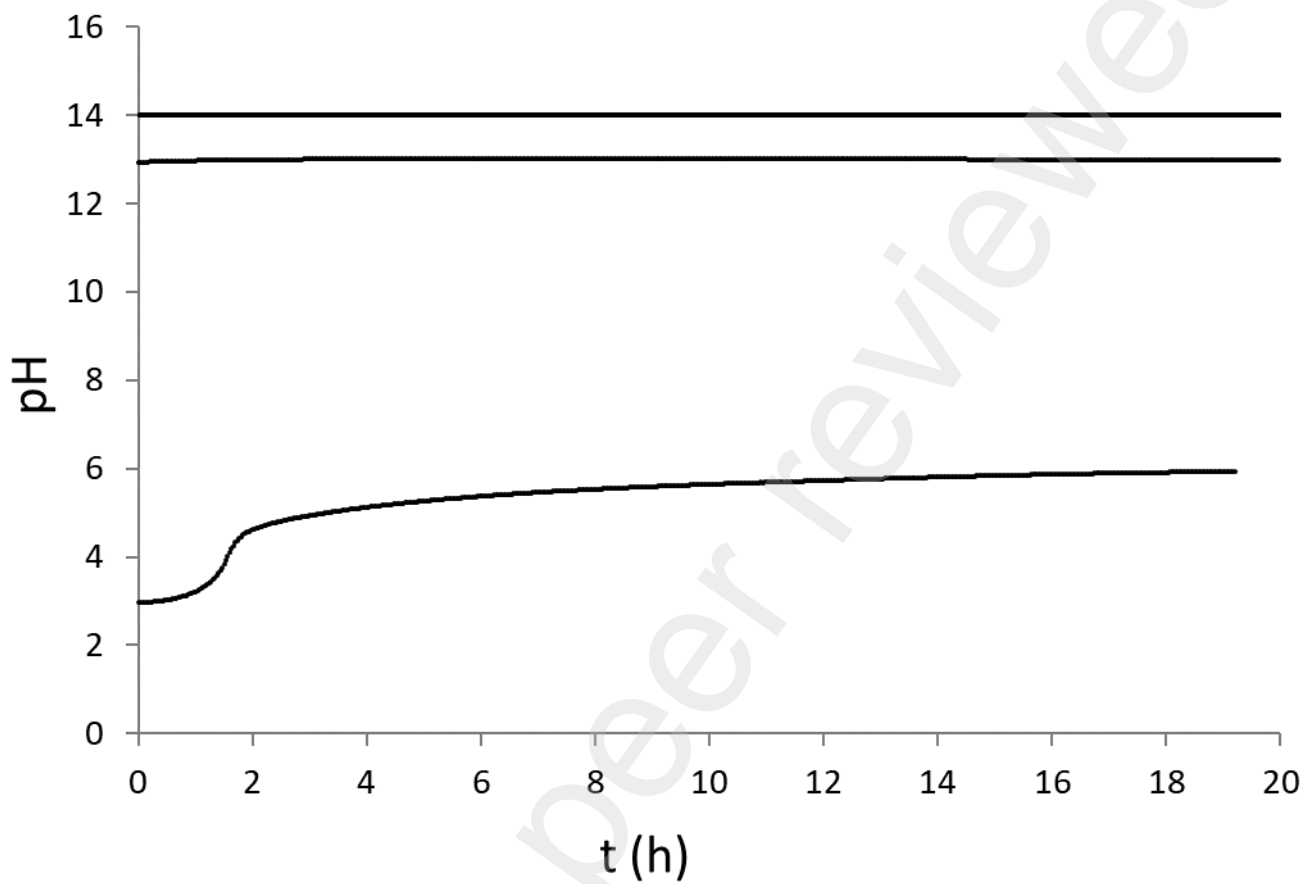


Figure 4: Experimental (points) and simulated (lines) impedance diagrams (Nyquist and Bode-Phase) recorded at OCP on Be electrode in aqueous solutions with various pH.

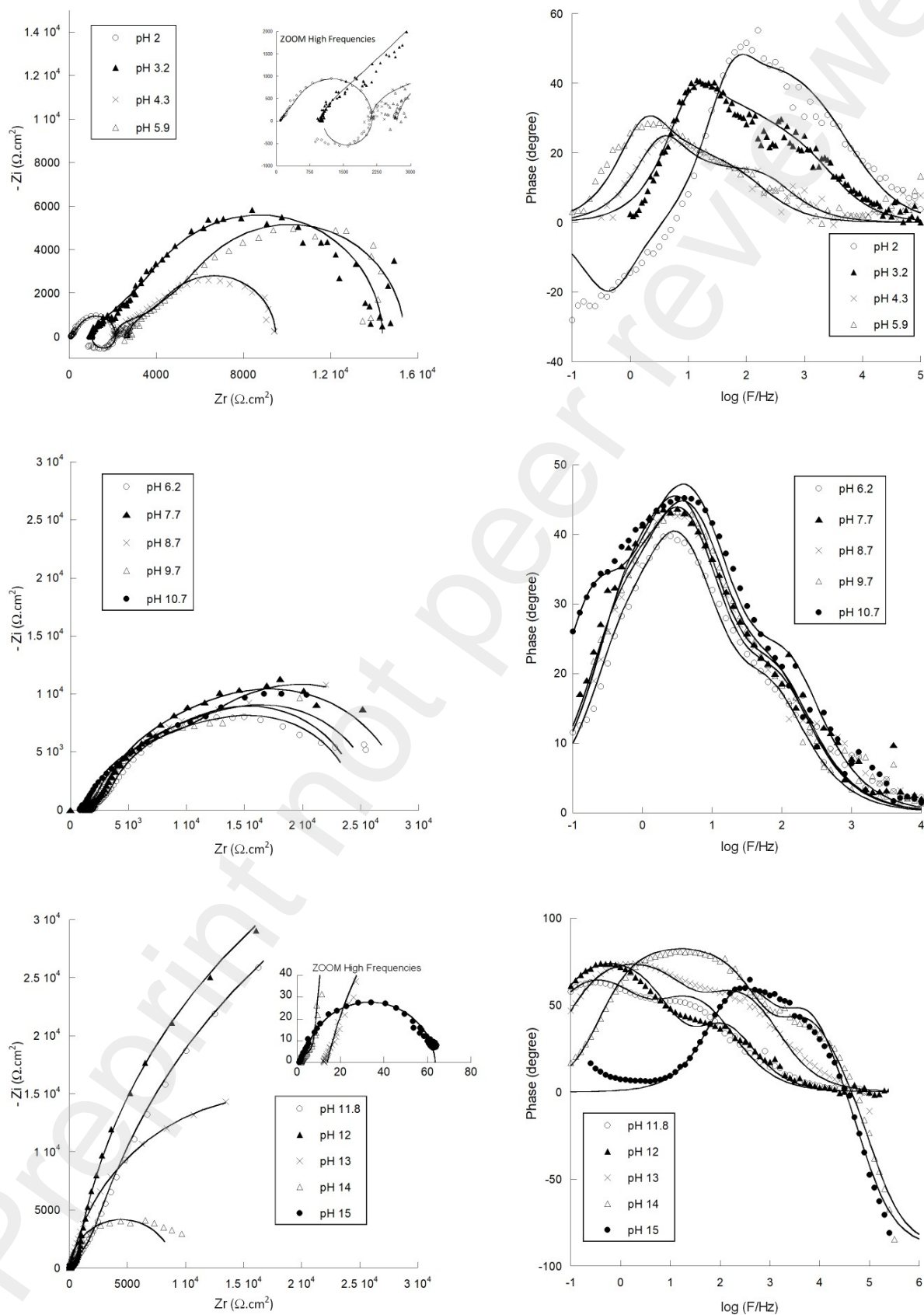


Figure 5: Equivalent electrical circuit used to fit the EIS diagrams recorded on a beryllium electrode in aqueous solution at different pH

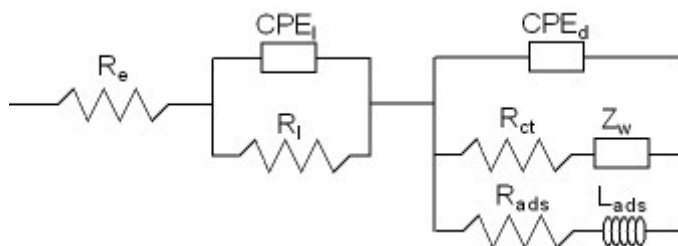


Figure 6: Variation of the charge transfer resistance calculated by electrical simulation of the electrochemical impedance spectra recorded on a beryllium electrode in aqueous solution at different pH. Superposition of the solubility values of $\text{Be}(\text{OH})_2$.

